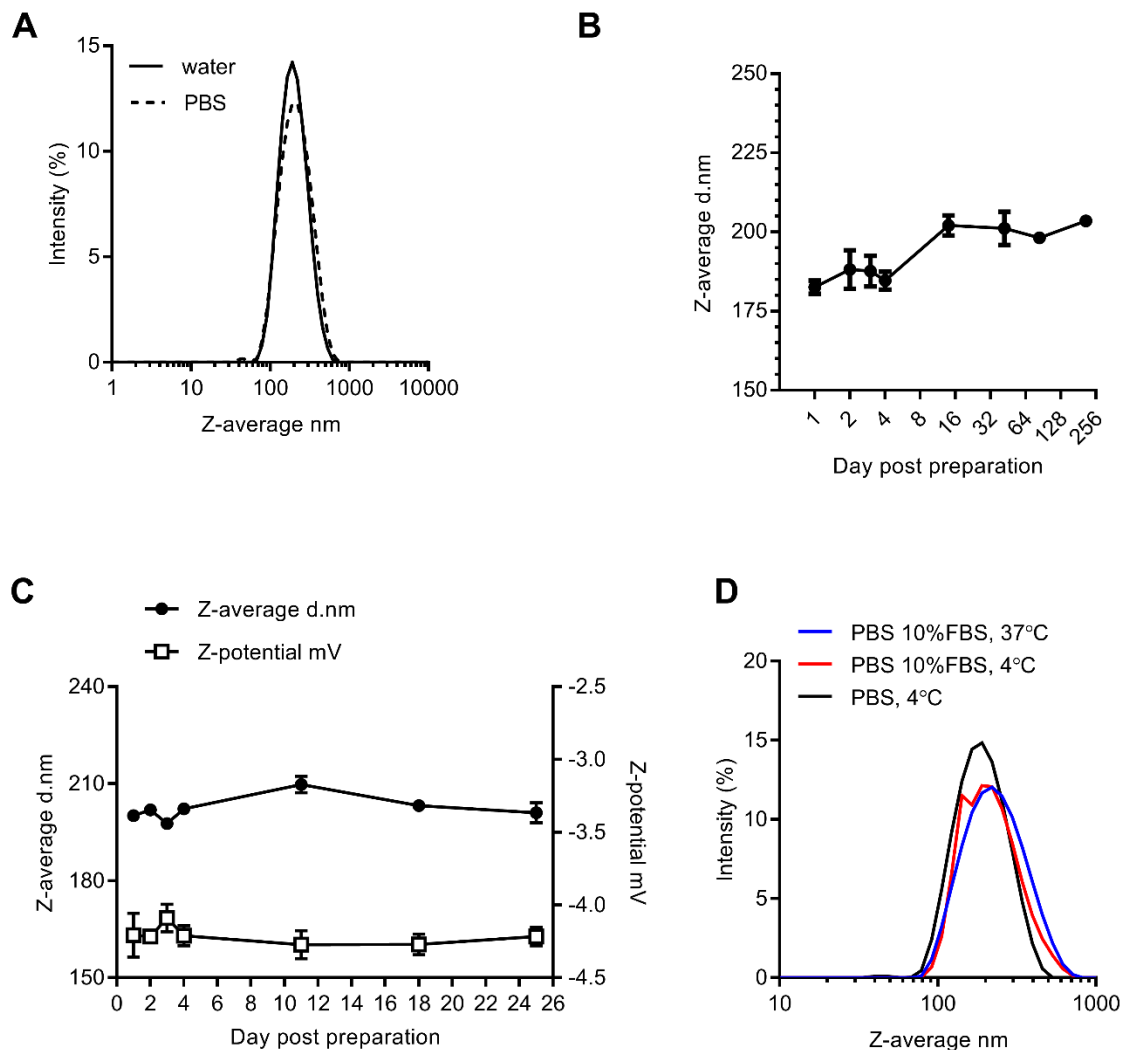
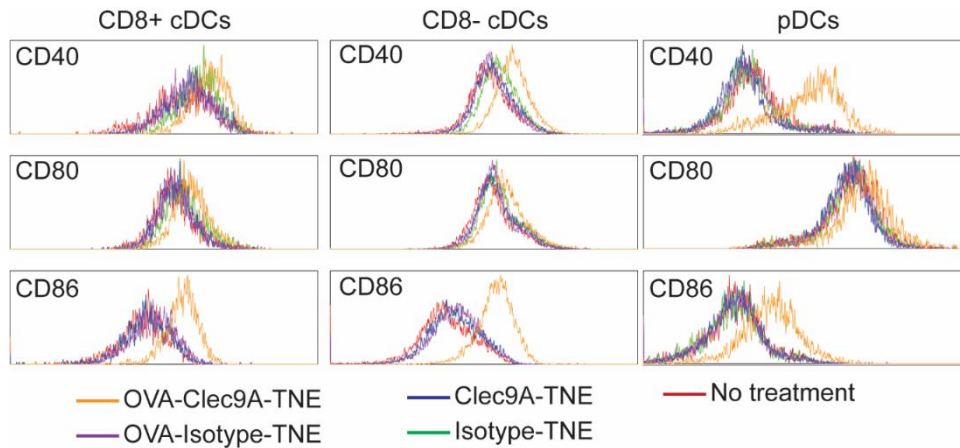


Supplementary figures



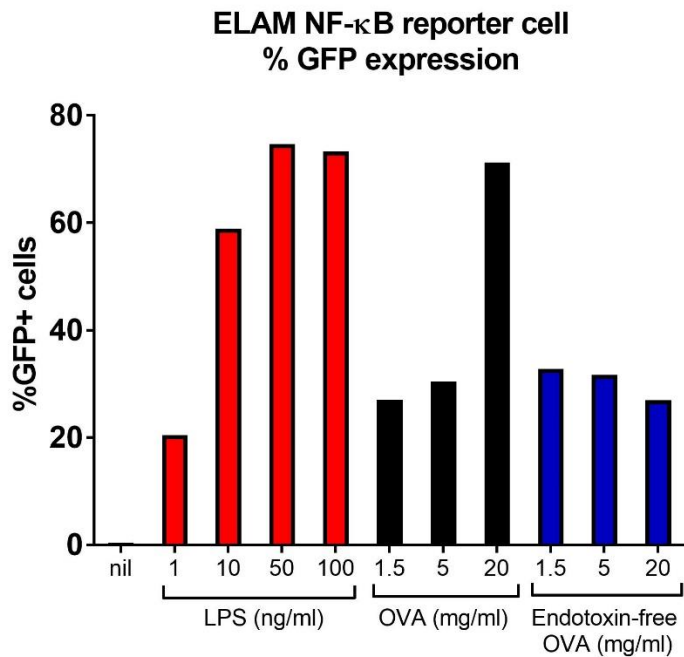
Supp. figure 1. TNE characteristics

(A) Particle size distribution of OVA-Clec9A-TNE diluted in water and PBS; (B) OVA-Clec9A-TNE were stored at 4 °C for over 256 days. Aliquots were removed periodically and diluted 1:100 in PBS for size measurement. (C) OVA-WH-TNE were diluted 1:100 in PBS containing 10% FBS and stored at 4 °C. Aliquots were removed periodically for size and zeta potential measurements. Data represent mean of three individual measurements with SD. (D) OVA-WH-TNE were diluted 1:100 in PBS or PBS containing 10% FBS and stored at 4 °C, or diluted 1:100 in PBS containing 10% FBS and incubated at 37 °C. Sixteen hours later, aliquots were removed for size measurements. Data represent mean of three individual measurements.



Supp. figure 2. OVA delivered by Clec9A-TNE promote DC activation.

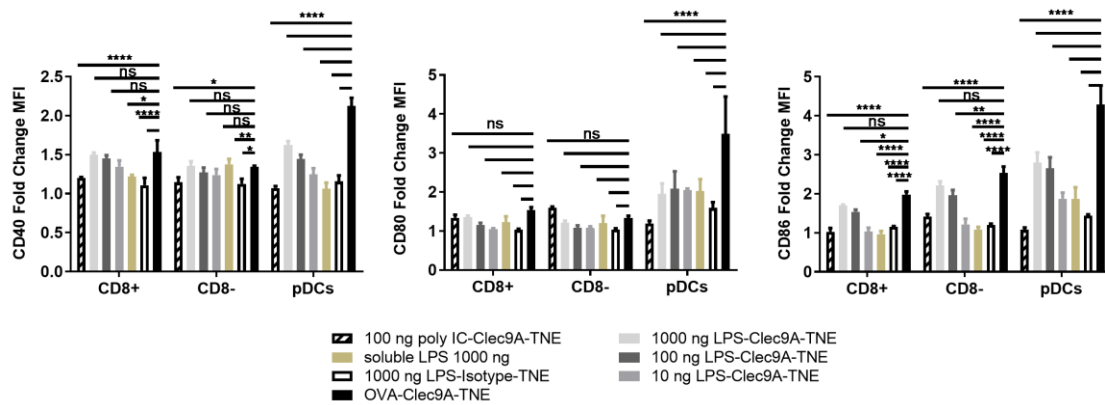
C57Bl/6 mice were injected i.v. with OVA-Clec9A-TNE, OVA-Isotype-TNE, Clec9A-TNE, or Isotype-TNE. Six hours later, surface expression of CD86, CD80 and CD40 by CD8+ DCs, CD8- DCs and pDCs was analyzed by flow cytometry. Representative histogram from two separated experiments are shown (n=6).



Supp figure 3. OVA but not endotoxin-free OVA induces NF- κ B transcriptional activity.

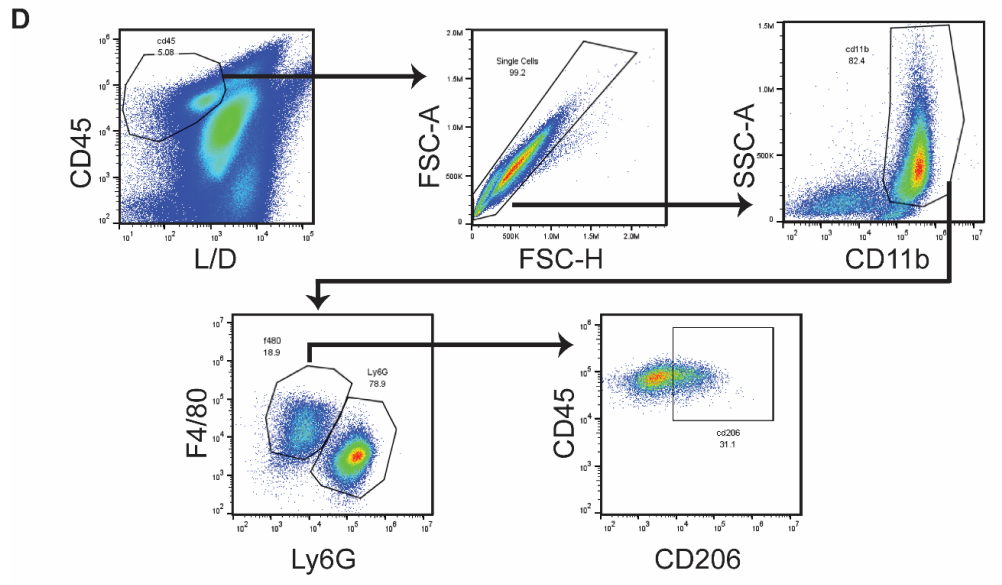
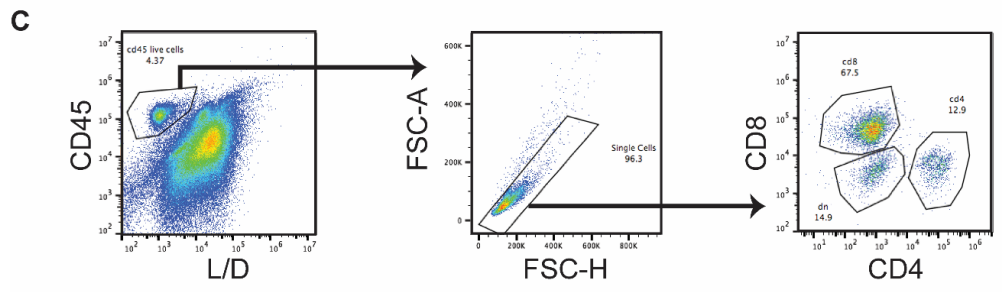
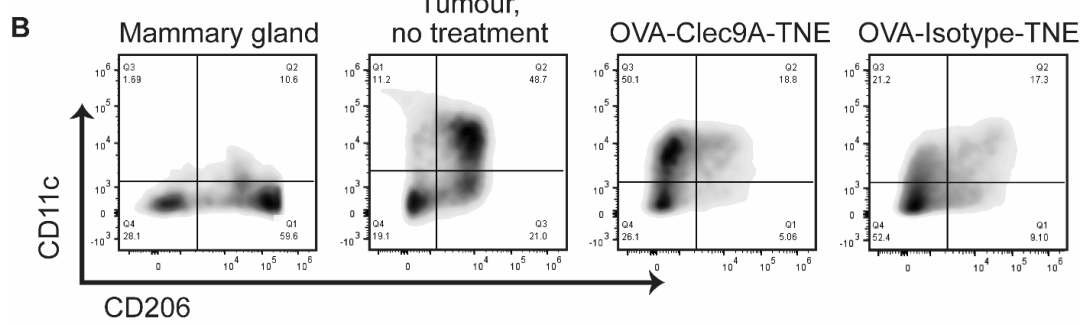
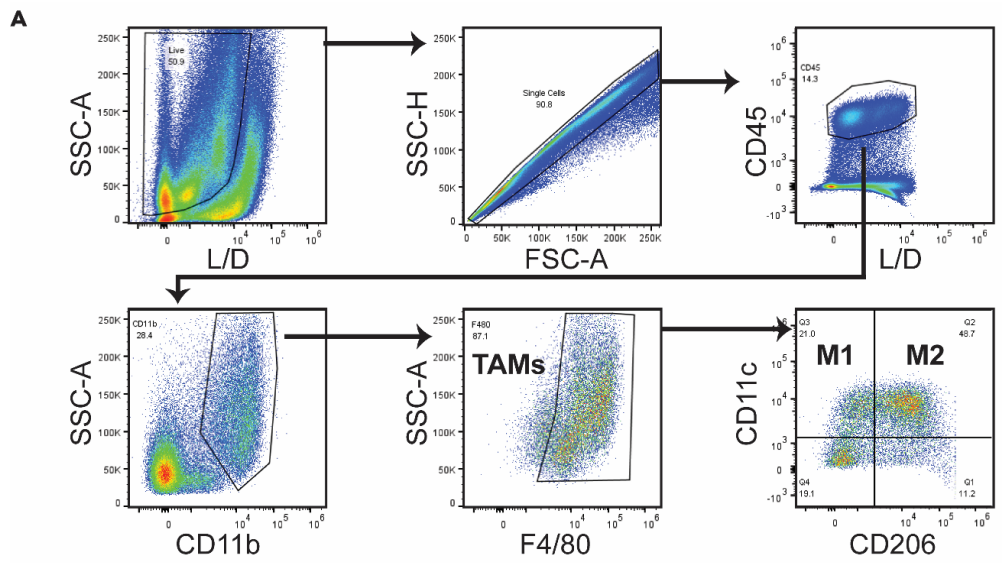
Detoxi-Gel Endotoxin Removal Gel (Thermo Scientific) was used to remove endotoxin from Ovalbumin (OVA, Sigma-Aldrich). RAW 264.7 mouse macrophages stably transfected with the endothelial cell-leukocyte adhesion molecule (ELAM) promoter controlling expression of

green fluorescence protein (GFP)-NF- κ B were cultured with either medium (nil), OVA, endotoxin-depleted OVA or LPS (*E.coli* Serotype O111:B4, Enzo) at the indicated concentrations for 4 hours. Cells were washed, stained with Live/Dead Fixable Near-IR Dead Cell Stain then analyzed for GFP positive live cells.



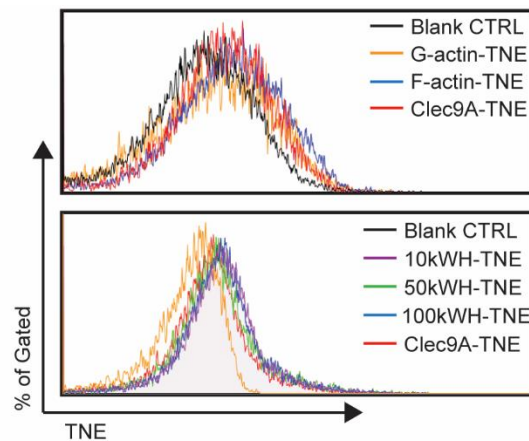
Supp. figure 4. Clec9A-TNE encapsulating poly I:C or LPS in the absence of antigen activated DCs much less effectively than OVA-Clec9A-TNE.

C57Bl/6 mice were injected i.v. at the indicated dosage of poly IC-Clec9A-TNE, LPS-Clec9A-TNE or LPS-Isotype-TNE. Six hours later, surface expression of CD86, CD80 and CD40 by CD8+ DCs, CD8- DCs and pDCs was analyzed by flow cytometry (n=3).



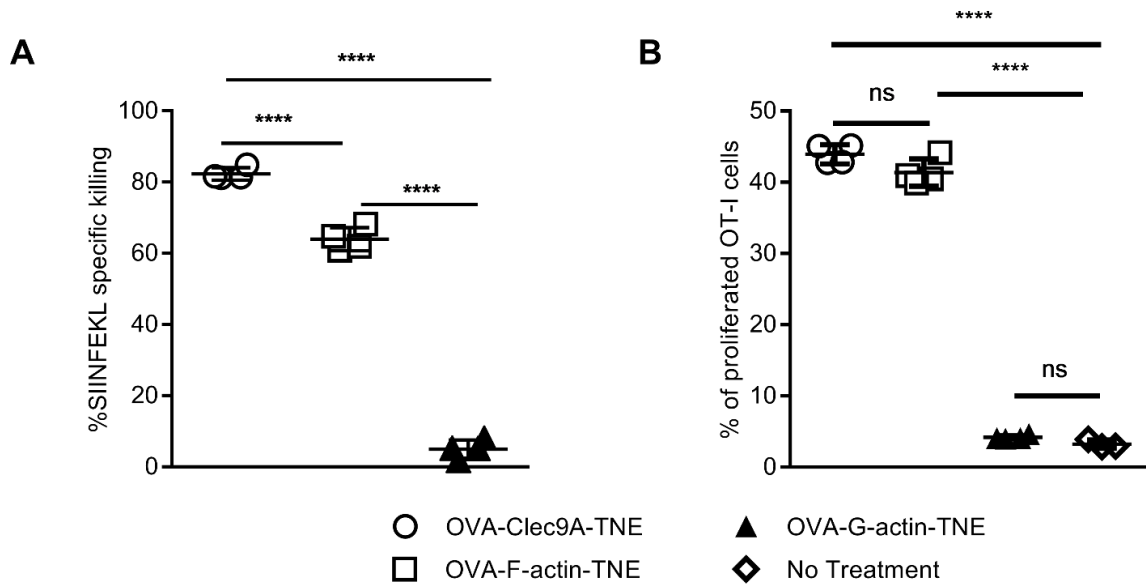
Supp. figure 5. Gating strategies for flow cytometry analysis.

(A) Representative gating strategy for tumor myeloid cells of C57BL/6 mice developing tumor after orthotopic injection of PyMT-mChOVA. This gating strategy was used in Figure 4b. (B) Representative cytogram showing M1 and M2 macrophage populations in the mammary gland of naïve C57BL/6, or PyMT-mChOVA tumor-bearing mice receiving OVA-Clec9A-TNE, or OVA-Isotype-TNE or left untreated. This gating strategy was used in Figure 4b. (C) Representative T cell gating strategy for the tumors of PyMT-mChOVA tumor-bearing mice. This gating strategy was used in Figure 4C and D.



Supp. Figure 6. In vivo specificity of Clec9A targeting TNE.

Same experiment as in Fig. 4E, histograms show actin-functionalized TNE (upper panel) and WH peptide-functionalized TNE (lower panel) binding and uptake by CD8+ cDCs.



Supp. Figure 7. OVA delivered by F-actin-TNE induced antigen specific killing and T cell response.

(A) C57BL/6 mice were adoptively transferred with equal numbers of unpulsed CTV^{low} and SIINFEKL-pulsed CTV^{high} target cells 6 days after i.v. injection with OVA-Clec9A-TNE, OVA-F-actin-TNE or OVA-G-actin-TNE. The percentage of SIINFEKL peptide-specific lysis in spleen is depicted (n=5). (B) CTV-labeled spleen cells from OT-I transgenic mice were transferred to C57BL/6 mice. One day later these mice were injected i.v. with 200 μ l of OVA-Clec9A-TNE, OVA-G-actin-TNE or OVA-F-actin-TNE (formulated with 5 μ g of OVA). Six days later, Spleens were removed and cell suspensions stained with anti-CD3 and CD8 were analyzed by flow cytometry. CD3⁺CD8⁺CTV⁺ cells were gated (n=4).